Calibration of Aeroelastic Prediction Methods: Comparison with Experimental Results on a Single Stage Compressor Blisk

Jean-Pierre LOMBARD, Virendra SHARMA, Jérôme DUPEUX, Michel DUMAS, Christian DUPONT
Snecma – Safran Group
Site de Villaroche
F-77550 MOISSY-CRAMAYEL
FRANCE

jean-pierre.lombard@snecma.fr / virendra.sharma@snecma.fr / jerome.dupeux@snecma.fr / michel.dumas@snecma.fr / christian.dupont@snecma.fr

Eric SEINTURIER
Turbomeca – Safran Group
Site de Bordes
F-64511 BORDES Cedex
FRANCE

eric.seinturier@turbomeca.fr

ABSTRACT

This paper presents a comparison between the measured and computed forced response of a high-pressure compressor Blisk for aeronautical applications. Measurements were carried out by ONERA on a Turbomeca transonic compressor. This test case provides reference experimental results against which simulation tools can be validated and calibrated for forced response analysis. The instrumented rotor was excited by the wakes from struts upstream of the blades. Simulations were carried out using unsteady Reynolds-Averaged Navier-Stokes (RANS) and 3D Euler codes at the test conditions. Blade mistuning was characterized by partial tests and introduced into the mechanical model. The Blisk's mistuned forced response were computed at the experimental gauges position and compared with the test results. Simulation predictions compare very well with the experimental results and these results are discussed.

KEY-WORDS

turbomachinery, HP compressor, aeroelastic coupling, unsteady aerodynamics, forced response, mistuning

1 INTRODUCTION

Aeronautical turbomachinery manufacturers seek to optimize their product designs in order to increase performance in terms of thrust, fuel consumption, operability and lifetime. From the mechanical design aspect, these efforts result in designs that are "fine-tuned" on the basis of prior experience, with more

Lombard, J.-P.; Sharma, V.; Dupeux, J.; Dumas, M.; Dupont, C.; Seinturier, E. (2005) Calibration of Aeroelastic Prediction Methods: Comparison with Experimental Results on a Single Stage Compressor Blisk. In *Evaluation, Control and Prevention of High Cycle Fatigue in Gas Turbine Engines for Land, Sea and Air Vehicles* (pp. 28-1 – 28-18). Meeting Proceedings RTO-MP-AVT-121, Paper 28. Neuilly-sur-Seine, France: RTO. Available from: http://www.rto.nato.int/abstracts.asp.

Report Documentation Page

Form Approved
OMB No. 0704-0188

1. REPORT DATE	2. REPORT TYPE	3. DATES COVERED
01 OCT 2005	**N/A**	**-**

4. TITLE AND SUBTITLE
Calibration of Aeroelastic Prediction Methods: Comparison with Experimental Results on a Single Stage Compressor Blisk

5a. CONTRACT NUMBER
5b. GRANT NUMBER
5c. PROGRAM ELEMENT NUMBER

6. AUTHOR(S)

5d. PROJECT NUMBER
5e. TASK NUMBER
5f. WORK UNIT NUMBER

7. PERFORMING ORGANIZATION NAME(S) AND ADDRESS(ES)
Snecma Safran Group Site de Villaroche F-77550 MOISSY-CRAMAYEL FRANCE

8. PERFORMING ORGANIZATION REPORT NUMBER

9. SPONSORING/MONITORING AGENCY NAME(S) AND ADDRESS(ES)

10. SPONSOR/MONITOR’S ACRONYM(S)

11. SPONSOR/MONITOR’S REPORT NUMBER(S)

12. DISTRIBUTION/AVAILABILITY STATEMENT
Approved for public release, distribution unlimited

13. SUPPLEMENTARY NOTES
See also ADM202115, RTO-MP-AVT-121. Evaluation, Control and Prevention of High Cycle Fatigue in Gas Turbine Engines for Land, Sea and Air Vehicles., The original document contains color images.

14. ABSTRACT

15. SUBJECT TERMS

16. SECURITY CLASSIFICATION OF:			17. LIMITATION OF ABSTRACT	18. NUMBER OF PAGES	19a. NAME OF RESPONSIBLE PERSON
a. REPORT	b. ABSTRACT	c. THIS PAGE			
unclassified	**unclassified**	**unclassified**	**UU**	**18**	

Standard Form 298 (Rev. 8-98)
Prescribed by ANSI Std Z39-18

particularly a large reduction in the number of mechanical connections between components. Some turbofan engine bladed disks – mechanically the most heavily loaded components - are now commonly produced as one-piece components. In this case one talks of IBR (Integrally Bladed Rotor) or Blisk (Bladed Disk) or Bling (Bladed Ring). The conventional bolted assemblies between bladed rotors give way to continuous connections obtained by inertia friction welding, for example. This progress in the fabrication and machining processes brings significant weight savings compared with conventional technologies and, to a lesser extent, improved aerodynamic performance of the engine. Conversely, the reduction in the number of mechanical connections generates a substantial reduction in the damping of the engine and the creation of greater dynamic couplings between components, not observed previously. The development of these technologies therefore poses new vibration problems to turbomachinery designers.

In this context, it is now more important than ever for engine manufacturers to have reliable tools to predict the dynamic behavior of their machines, and to have them as early as possible in the design phase in order to prevent problems of vibration fatigue and the ensuing costly redesigns.

The sources of excitation of a turbomachine are essentially of aerodynamic origin. To counter two major problems, Snecma has developed a specific tool to predict the aeroelastic behavior of blisks:

- **Synchronous forced response:** Any asymmetry in the aerodynamic flowpath constitutes a potential synchronous excitation of the speed of rotation (upstream or downstream fixed blades, structural arms, air tapping orifices, injectors, air intake duct distortion induced by a flight with angle of attack or crosswind, etc.). The designers seek to avoid situations of frequency coincidence between a bladed disk mode and a harmonic of the engine speed in the usual engine operating ranges (one talks of a frequency margin). The design constraints however are such that it is sometimes difficult if not impossible to respect these criteria. It is therefore crucial to be able to estimate the forced vibration response levels generated by these coincidence situations. After superpositioning the dynamic loads on the static loads (generated by the centrifugal forces, the effects of thermal expansion and the steady aerodynamic thrust), knowing the total mechanical loading enables the component to be situated with respect to its endurance limit.
- **Asynchronous free response:** Another problem concerns the problems of stability (flutter) of the blisks. Under certain aerodynamic conditions, very small amplitude blade movements can become considerably amplified to a level stabilized by structural or aerodynamic non-linearities (here one talks of a limit cycle) or to a level leading to rupture of a component. The flutter analysis leads to the estimation of the total damping of the aeroelastic system (mechanical plus aerodynamic damping) and enables the component's margins to be displayed with respect to a situation of potential instability.

These two analyses are carried out with an approach of weak coupling between the structure and the fluid (this approach is justified by the light fluid hypothesis). The prediction’s quality is dependent on correctly estimating the aerodynamic excitation and damping forces. Likewise, taking into account the mistuning (frequency differences between blades induced by the dimensional and material scatter) influences the response levels through localization effects [1]. Considerable work has been performed to improve predictions of the unsteady aerodynamic forces applied to the blades and the mistuning phenomenon. The present study concerns the calibration of these aeroelastic prediction tools as a preliminary step before their industrialization and their use in the design cycle.

2 PRESENTATION OF THE TEST RIG AND CONFIGURATION

The test bench (Figure 1) at ONERA consists of a rotor/blade assembly of a Turbomeca transonic axial compressor. It is an Integrally Bladed Rotor (IBR), or blisk, with 23 blades, driven mechanically by ancillary

equipment. In the configuration presented here, the blisk spins at about 30,000 rpm downstream of a stator comprising 9 vanes (Figure 1). The vibration phenomenon studied corresponds to the synchronous response of the IBR to the aerodynamic excitations induced by the passing wakes from the upstream stator. Near maximum rotation speed, resonance of the blades on their 3rd mode (2^{nd} bending of blade) is observed and its frequency coincides with harmonic 9 of the rotation speed (Figure 2).

The observations on the configuration are obtained chiefly through total pressure sensors rakes and dynamic strain and unsteady pressure gauges mounted on the IBR blades. A precise characterization of the flow structure has also been carried out using the PIV (Particle Image Velocimetry) technique. The steady aerodynamic conditions in the test flowpath were finely characterized to permit precise calibration of the aerodynamic field by the steady simulations.

The modal parameters of the IBR were identified by partial tests at several stages of the instrumentation installation procedure: the blade frequencies and modal damping were characterized. The distortion gauges mounted on the IBR blades underwent a calibration procedure: measurement of the correspondence between the modal strains at the gauge and the modal velocities at the blade tip obtained by laser velocimeter.

3 METHODOLOGY

3.1 General methodology

The procedure used to predict the forced response consists firstly in identifying the vibration risk through the Campbell's diagram (Figure 2). The selected rotation speed determines the aerodynamic conditions for which the forced response study must be performed. Three steps are required to make the aerodynamic analysis. The first consists in calibrating the predicted steady aerodynamic field to be situated as close as possible to true conditions. This calibration is achieved through precise positioning in the overall performance diagram (compression ratio – flow rate) of the engine. More accurate calibration with other measured aerodynamic quantities (radial pressure distributions, flow angle, Mach number, etc.) can also be performed if the data are available. The next stage consists in performing an unsteady calculation from this steady aerodynamic field. The unsteadiness of the flow is generally related to the passing wakes of the obstacle (stator) upstream of the studied rotor. This calculation provides the unsteady pressures on the surface of the blades necessary to estimate to generalized aerodynamic forces (GAF), obtained by calculating the products of these forces with the displacements of the mode corresponding to the coincidence. To predict the blade response, an estimate of the overall system damping, and in particular of the aerodynamic damping, must also be obtained. The aerodynamic damping requires an additional stability calculation using either a linearized method or a non-linear calculation.

3.2 Aerodynamics: steady modeling

The aerodynamics are modeled using 3D-compressible Reynolds-Averaged Navier Stokes (RANS) equations, averaged by the Favre technique and completed by a turbulence model. The turbulence is modeled by the k-ε model of Launder-Sharma with two transport equations for the turbulent kinetic energy (k) and its rate of dissipation (ε). These equations are solved by a finite volumes method associated with a time-marching technique. The spatial discretization uses Van Leer splitting and 3rd-order precision MUSCL extrapolations techniques. To save computational costs, the bladed disks are calculated over a sector of the blade. The flow is considered periodic in the azimuthal direction. A detailed description of the modeling and numerical techniques used is given in [2].

The computational code used is associated with a multi-block mesher using H and O topologies. The blades are discretized by means of an O meshing, while the H meshings are used to discretize the upstream and downstream domains of the blades. The rotor clearance at the blade tips is also discretized using O meshings [2]. Single-channel modeling imposes the use of the "mixing plane" technique to take into account the multi-rotor environment. This technique exchanges conservative aerodynamic quantities averaged azimuthally at each radius of the plane common to two adjacent blades in the O meshing [3].

3.3 Aerodynamics: unsteady modelings

The quantities sought are the first unsteady pressure harmonics generated by the passing wakes of the obstacle upstream of the blade and the value of the aerodynamic damping.

3.3.1 Unsteady exciting pressures

Two different methods were used to obtain unsteady pressures on the blade. The first consists in solving the unsteady 3D Navier Stokes equations for the complete stage (upstream strut and rotor). The second uses an upstream limit wake condition on an isolated unsteady rotor; the wakes are obtained from 3D steady NS calculations. The unsteady computations are carried out on a single channel, like the steady calculation. The Euler method requires prior 3D steady Euler calculations that serve as an initialization for the unsteady part. These calculations have to be calibrated with respect to the 3D NS calculations providing the exciting wakes in order to obtain comparable aerodynamics.

The unsteady 3D NS method on the complete stage has the advantage of being much more precise, but the computational cost is much higher. The calculation cost can be reduced by using a time-space flow phase lagged boundary conditions (chorochronicity) that allows the resolving of each assembly of blades on a single channel [4]. The calculation cost is also reduced by using a dual time step technique that speeds up the convergence.

3.3.2 Unsteady damping pressures

Two methods have also been used to estimate the aerodynamic damping of the system. The first solves the non-linear 3D Euler equations with an imposed meshing movement corresponding to the studied mechanical mode. The second uses a 3D Navier Stokes simulation that is linearized in time, also with a meshing movement following movements imposed by the mechanical mode [5]. The Navier–Stokes method is more costly in computation time but allows for viscous effects - which are very important in turbomachinery flows - to be taken into consideration.

3.4 Mechanical model

The conservative mechanical behavior of the studied disk is conventionally obtained from an FE (Finite Element) model with cyclic symmetry of a blade plus disk sector (Figure 3). This approach brings a huge saving in computation time and storage costs compared with the use of a complete bladed disk model (360°). A Benfield and Hruda component mode substitution method is then used to describe the overall behavior of the bladed disk in the presence of mistuning [6] [7] (a detailed description of the method is given in [8]). The disk is chosen as a central sub-structure and the blades as satellite sub-structures. This sub-structuring allows the introduction of a mistuning pattern localized on the blades. This mistuning can be frequency related (as in the case presented), but the method is also validated for the use of form mistuning if this has to be taken into account (prediction of the aeroelastic behavior after accidental events such as bird or ice ingestion). The results obtained for the simulated response of a turbine stage are shown in [8].

Other methods of simulating these phenomena are proposed in the literature [9] [10]. The same reduced-order model is used to predict the stability of the blisk in the presence of unintentional [11] or intentional mistuning [12]. The generalized reduced-order model is systematically validated with respect to predictions obtained with the reference model with cyclic symmetry. The criteria for validating the reduced-order model concern the prediction of eigensolutions and the forced response to point mechanical excitation in the frequency range of interest (Figure 4).

3.5 Mistuned aeroelastic coupled reduced-order model

After reduction by modal synthesis, the aeroelastic coupled problem fits into the space of generalized coordinates in the frequency domain via the relation:

$$\left[\overline{K} + \overline{K}^{mistun} + \overline{A}^{aero} + j\left(\overline{B}^{aero} + \overline{K}^{hyst}\right) - \omega^2\,\overline{M}\right] q(\omega) = \bar{f}^{aero}(\omega)$$
$$y(\omega) = P\,q(\omega)$$

where: $\overline{K}, \overline{M}$ generalized matrices of stiffness and mass of the bladed disk

$\overline{K}^{hyst}, \overline{K}^{mistun}$ generalized matrices of mechanical damping and mistuning

$\overline{A}^{aero}, \overline{B}^{aero}$ generalized matrices of aerodynamic damping

$q, \bar{f}^{aero}$ generalized displacement and aerodynamic excitation force vectors

y, P physical displacement vector and problem reduction matrix

ω system excitation pulse

This reduced-order model is valid in a rotation speed range close to the operating speed at which the structure and the applied aerodynamic loads are calculated. The term mechanical damping is introduced into the problem reduced to a hysteretic form equivalent to the identified modal damping. The identified frequency mistuning is obtained by disturbing the generalized stiffness matrix only on the modal degrees of freedom associated with the blade modes. The aerodynamic damping is taken into account in the reduced-order model; the eigenvalues of the coupled free system are very slightly affected compared with the eigenvalues of the mechanical system, this being consistent with the chosen light fluid hypothesis. The reduced problem is solved by direct reversal at each frequency step or by calculation and superpositioning of the modes of the reduced dissipative system. The harmonic responses on the desired physical degrees of freedom (on the blade displaying the highest level for example) are restored via the reduction basis and the associated stress field is then deduced.

4 APPLICATION TO THE TEST CONFIGURATION AND CORRELATION

The methodology described in section 3 is applied to the test configuration with a view to validating the 3D Euler and 3D Navier-Stokes methods. The stage unsteady 3D NS calculation must serve as a reference for the

calibration of the Euler method. In effect, at present only the Euler methodology can be envisaged for calculating aerodynamic excitation pressures in a design cycle due to its speed and lower computation cost. A meridian view of the geometry of the test aerodynamic flowpath is shown in Figure 5.

4.1 Aerodynamic calibration: steady-state

The availability of detailed measurements as radial distributions of the total pressure, the Mach number and the flow angle in the planes upstream and downstream of the rotor allow precise calibration of the steady solution. The predictions on the 3D NS stage configuration were made on a 3-million-point mesh shown in Figure 6A. Figures 6 - 8 summarize the results of this calibration. Figure 6B shows the flow structure through entropy contours at 90% of the blade span. The importance of the flow separation on the suction side of the stator vanes upstream of the wakes generated by the high setting angle of the blades is clearly visible. The effect of the mixing plane is also clearly visible: the flow becomes uniform on entering the rotor domain, the wakes having been mixed out by the averaging effect. This justifies the unsteady approach (stator plus rotor) used subsequently to simulate the interaction between the wakes and the rotor, even though it is costly in computation time.

The calibration in terms of global performance (Figure 7) shows good agreement with the test results (less than 3.4% in compression ratio and 5% in flow rate) for the 3D NS stage calculations. The agreement is confirmed by the calculation/test comparison downstream of the rotor (Figure 8). Figure 7 also shows the results from 3D Euler and 3D NS modelings on an isolated disk using the radial distributions of angle, total pressure and Mach number measured upstream of the rotor during tests as limit input conditions. These calculations are necessary with Euler modeling to apply the method of passing wakes, and in 3D NS modeling for the aeroelastic damping computations.

4.2 Unsteady calculations

The steady calibration on the stage configuration allows the operating point to be chosen for the reference unsteady 3D NS calculation. The operating point was chosen (Figure 7) with respect to the measured compression ratio. Considering the size of the meshing used, the calculation costs are extremely high: 220 hours CPU time on a Fujitsu VPP5000 vector supercomputer were necessary to attain 44 periods of passing of exciting wakes. A sampling rate of 144 time steps per period was used. The effect of taking into account flow unsteadiness is a change in the operating point (Figure 7). In effect, the mean value of the global performance of the machine is affected with respect to the corresponding steady calculation. The differences are of –0.62% in flow rate and –0.5% in compression ratio. This is explained by the transmission of the wakes across the interface between the two rotors (Figure 9) and the interactions between the wakes and the boundary layers of the blades. This displacement of the operating point reduces the calculation/test differences.

The Euler 3D method is more economic in calculation time. This justifies its utilization in a design process in spite of its modeling limitations. A periodic solution is reached in 30 periods with a sampling of 64 time steps per period. The calculation cost is about 1h on a Fujitsu VPP300 or less than 15 minutes on a VPP5000.

Figures 10 and 11 show a comparison of the first harmonic of the unsteady pressures obtained by the two methods. The two methods show similar structures on the blade surfaces, but the 3D NS method nevertheless gives a more complex structure. In terms of level of the first pressure harmonic, the 3D NS method predicts values that are two times higher than the 3D Euler predictions on average.

The last step from an aerodynamic point of view is the estimation of the aeroelastic damping. The aeroelastic damping value obtained with the non-linear Euler method for the 3rd mode at –9 diameters is 0.26%. The linearized 3D NS method gives a value 0.31% higher for the same diameters mode.

4.3 Forced response calculations/test correlation

The FE model used was not subject to any specific corrections or updating. The predicted natural frequencies for the mode in question are slightly lower than those of the studied resonance. A mechanical reduced order model is built by modal synthesis and validated with respect to previously stated criteria (Figure 4). The error in natural frequency committed on the studied mode is less than 1/10000. This model has a size of 580 generalized degrees of freedom.

The unsteady aerodynamic pressure forces calculated by a Euler method for the operating point the closest to the test conditions are applied to the model, initially without mistuning. This choice is justified by the desire to validate aeroelastic tools in a design approach. The calculated aerodynamic damping (whatever the method used) is not used here because it is largely overestimated. The difference between the predicted level (Euler excitation) and the average of the viable measurements allows the downward readjustment of the mechanical damping identified during partial testing. This in fact translates an amplitude deficit in the predicted excitation pressures or a pressure field structure different to reality which has a lowering impact on the excitation GAF. This observation is corroborated by the 3D NS results.

To facilitate the correlation, particularly in terms of profile, the predicted responses form the subject of an offset in rotation speed common to all the blades. The results shown are generalized, but the abscissa of all the figures corresponds to the same rotation speed range; the resonance peaks observed on the gauges display different positions due to the natural mistuning. The position of these maxima is correlated with the introduced mistuning pattern: this indicates a low contribution of the disk in the mode shape considered (2F), consistent with the high number of diameters of the excited mode (9ϕ). The correlation is performed on the displacement amplitude of the responses. The signals measured on the distortion gauges are converted into displacements using the calibration relations measured in the partial tests and corrected by taking into account the static loads applied via the FE model. The measurements obtained from a slow rise in speed of rotation are subject to interference: with this type of test, it is difficult to perform repetitive tests due to the drift in aeroelastic behavior, and therefore it is difficult to perform averaging operations to reduce the measurement noise.

- **Sensitivity to the mistuning response:** Having 3 mistuning patterns (adjacent) identified at different stages of the bladed disk instrumentation (Figure 12), a mistuning response sensitivity analysis was carried out (Figure 13) with the damping identified in the partial tests. The results of this analysis show that the mistuning pattern is a first-order parameter in the estimation of response amplifications.
- **Forced response calculations/tests correlation:** A correlation between observed and predicted responses on 10 gauges positioned on 10 different blades is presented (Figure 14). The mechanical damping used for this correlation is that obtained after downward adjustment of the damping identified in the partial tests. The positions of the resonance peaks are consistent between gauges. The response profiles are located again. The response amplifications are correctly estimated and the blades displaying maximum levels are located.

5 CONCLUSIONS AND PROSPECTS

A method for predicting the aeroelastic response of a bladed disk taking mistuning into account was applied to a highly instrumented experimental configuration of a compressor stage representative of engine conditions.

A substantial amount of steady calibration using 3D NS tool was carried out and shows very good agreement between the computations and the tests, with respect to both the overall performance and the radial

distributions of aerodynamic quantities downstream of the rotor. Two methods were used to predict the unsteady pressure levels on the blades. An unsteady 3D NS calculation was performed on the complete stage and compared with a less costly method of passing wakes using unsteady Euler modeling. The two methods predict similar structures on the blade assemblies but the 3D NS calculations give unsteady pressure levels two times higher than those obtained with the 3D Euler calculations. Predictions of aerodynamic damping were also carried out with the linearized 3D NS method and non-linear 3D Euler method.

A reduced-order mechanical model obtained by modal synthesis was produced. This model allows the prediction of an aeroelastic behavior mistuned by disturbance of the natural frequencies of the blades. The prediction of this reduced order model was verified through comparison with cyclic symmetry calculations. The calculated aerodynamic damping turned out to have been overestimated therefore it was not introduced into the model for the prediction presented here. Only the mechanical damping identified during the partial dynamic test was introduced and adjusted accordingly in order to update the average response levels. The influence of the mistuned response was studied with mistuning patterns identified in the partial tests. For this type of poorly dampened IBR, the precision of the mistuning factor is of prime importance for quality of prediction. The results obtained at the gauges are highly satisfactory considering the noise level affecting the measurements obtained on the acquired rise in rating. The response profiles are found again along with the amplification levels.

Combined with the mistuning identification methods currently being industrialized at Snecma [13] [14], simulation of the mistuned response reveals itself as a precious tool for the engine vibration certification phases for integrally bladed rotors: the blades displaying maximum amplification levels are located and the engine gauge instrumentation can be positioned accordingly. Moreover, the flat-rate safety coefficients usually applied to the observed dynamic levels to take these amplifications into account can be adjusted by means of multiple random mistuned simulations.

The results can also be used to validate aerodynamic models to predict the aerodynamic excitation forces for this configuration. At present, this type of analysis is included in the engine development phases.

A prospective research possibility concerns the simulation of the excitations generated by the blades furthest from the excited bladed disk and whose wakes are affected by the intermediate vane assemblies. This necessitates multi-stage unsteady aerodynamic analyses. Another aspect is to focus on non-synchronous flow vibration. The reduction in the unsteady aerodynamic calculation costs is also a major avenue for improvement. Another important development objective in view of the evolution of turbomachinery design is the inclusion of the dynamics of adjacent disks in the mechanical model. Lastly, the development, qualification and industrialization of non-linear point or peripheral friction models are continuing, with concern for compatibility with the aeroelastic behavior prediction tools.

We would like to thank our partners at Turbomeca and Onera who helped carry out these aeroelastic tests.

BIBLIOGRAPHY

[1] **M.J Kruse, C. Pierre**, "Localization in bladed disks, part II: forced response", ASME 97-GT-502, ASME Gas Turbine Conference, 1997, Orlando, Florida.

[2] **G.A Gerolymos, G. Tsanga, I. Vallet**: “Near Wall k-ε Computational of Transonic Turbomachinery Flows With Tip Clearance” AIAA Journal, Vol. 36, 1998, pp. 1769-1777

[3] **G.A Gerolymos, C. Hanisch,** ″Multistage 3-D Navier-Stokes Computation of Off-Design Operation of a 4-Stage Turbine″, Imech J. Power energy, Vol.213, 1999, pp. 243-261.

[4] **C. Hanisch,** "Aérodynamique Numérique 3D instationnaire des turbomachines axiales", Thèse de l'Université Pierre et Marie Curie, Paris, novembre 1999

[5] **J.C Chassaing, G.A Gerolymos:** "Compressor Flutter Analysis using time nonlinear and time linearized 3D Navier-Stokes Methods", ISUAAAT, Lyon (France), 2000

[6] **M.P Castanier, G. Ottarsson, C. Pierre,** "A reduced order modeling technique for mistuned bladed disks", ASME Journal of Vibration and Acoustics, 1997, Vol. 119 (3), pp. 439-447.

[7] **M. Berthillier, C. Dupont, P. Chanez, F. Saurat,** "Réponse forcée aéroélastique des aubes de turbomachines", Revue Française de Mécanique, 1998, Vol. 1998/04.

[8] **E. Seinturier, J.P Lombard, M. Berthillier, O. Sgarzi,** "Turbine mistuned forced response prediction – Comparison with experimental results", ASME-IGTI Turboexpo GT-2002-30424, 2002, Amsterdam, The Netherlands.

[9] **R. Bladh, M.P Castanier and C. Pierre**, "Component mode based reduced order modeling techniques for mistuned bladed disks - Part I & II", Journal of Engineering for Gas Turbine and Power, 2001, Vol. 123, pp 89-108.

[10] **M.T Yang and J.H Griffin**, "A reduced order model of mistuning using a subset of nominal system modes", Journal of Engineering for Gas Turbine and Power, 2001, Vol. 123, pp. 893-900

[11] **E. Seinturier, C. Dupont, M. Berthillier, M. Dumas,** "A new method to predict flutter in presence of structural mistuning", congrès ISUAAAT, 2000, Lyon, France

[12] **J.P Lombard, J. Dupeux, C. Dupont, F. Garcin, S. Baumhauer,** "Mistuning phenomena on bladed disk: industrial methods and applications", submitted to ASME-IGTI Turboexpo GT-2006-90205, May 2006, Barcelona, Spain

[13] **F. Pichot, F. Thouverez, L. Jezequel, E. Seinturier,** "Mistuning parameters identification of a blisk", 4th International Conference On Damage Assessment Of Structures (DAMAS), Cardiff, 2001.

[14] **D. Laxalde, J.J Sinou, F. Thouverez, S. Baumhauer, J.P Lombard,** "Experimental identification of the mistuning of an industrial blisk", submitted to ASME-IGTI Turboexpo GT-2006-90569, May 2006, Barcelona, Spain

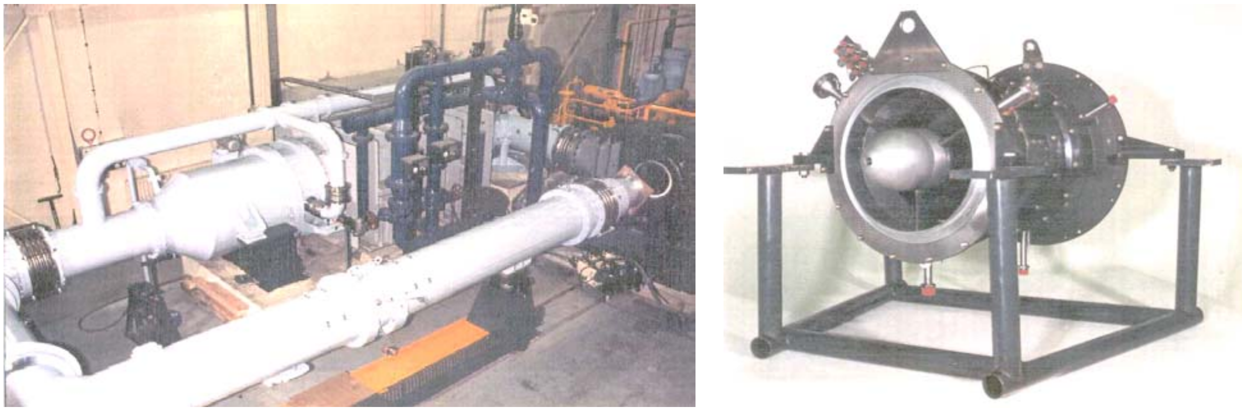

Figure 1: View of the test rig, tested compressor stage.

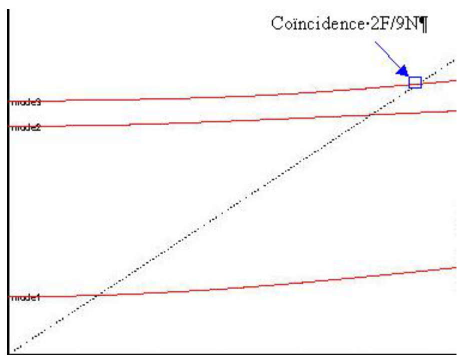

Figure 2: Campbell diagram (frequency / rotation speed) of the rotor.

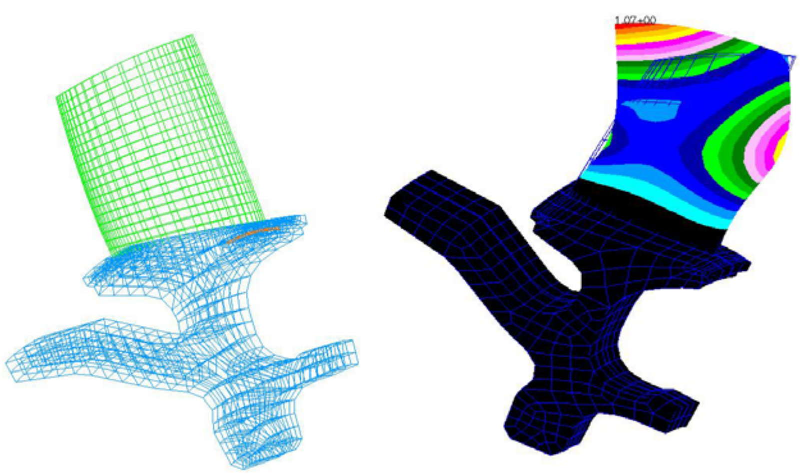

Figure 3: FE model of the blade disk sector - second bending mode of the blade.

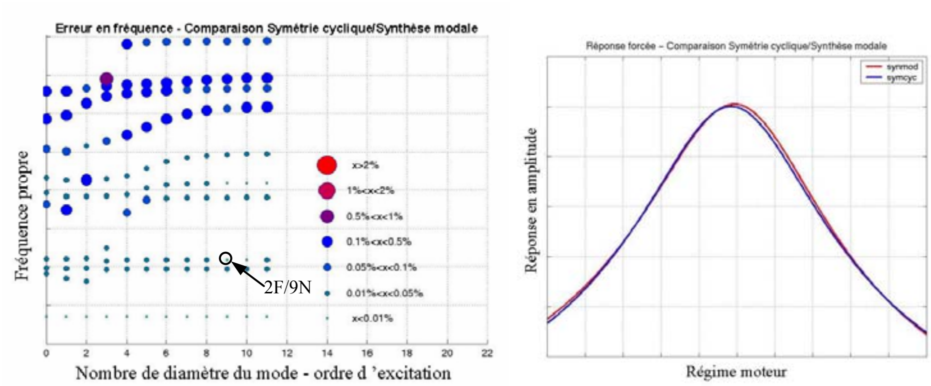

Figure 4: Qualification criteria for the reduced order model.

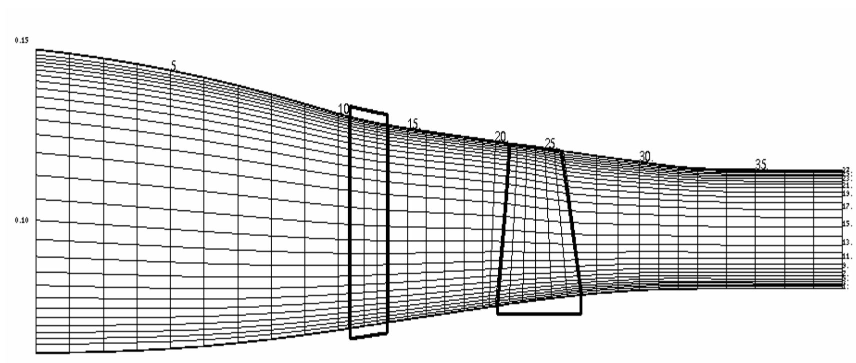

Figure 5: Meridian view of the experimental compressor aerodynamic flowpath.

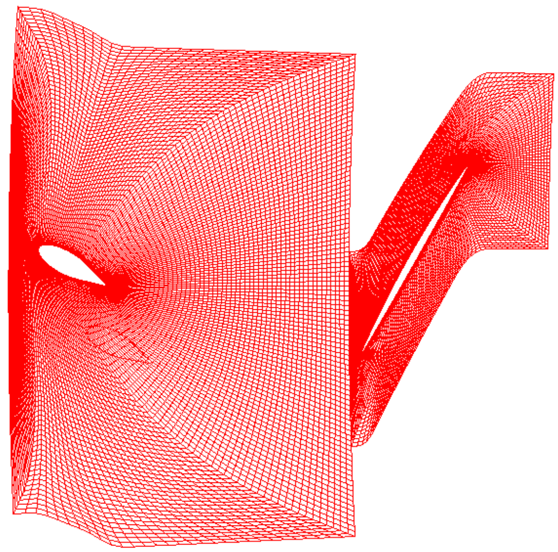

(A) View of the meshing at 90% of the height of the aerodynamic flowpath

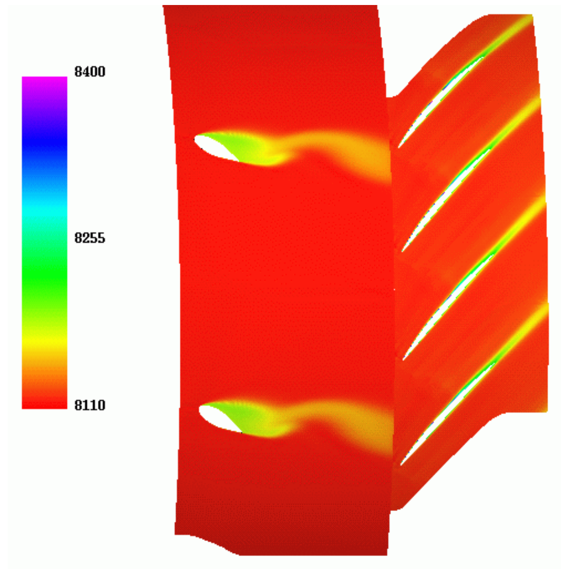

(B) Steady calculation result: iso-entropy at 90% of height of aerodynamic flowpath

Figure 6: 3D NS steady calculations: flow meshings and structure.

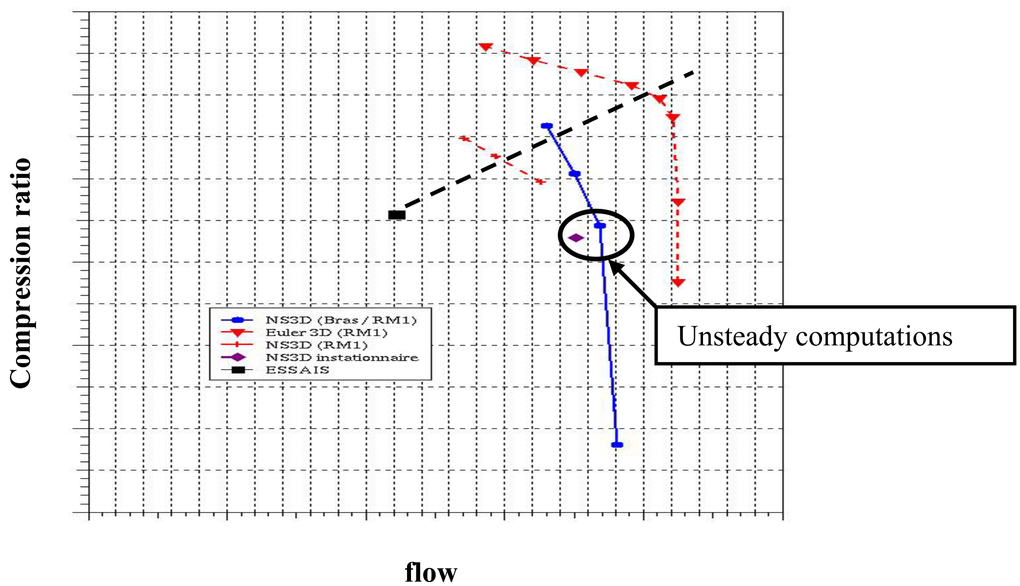

Figure 7: Calibration of steady calculations (3D NS and 3D Euler) with respect to the compression ratio / flow tests.

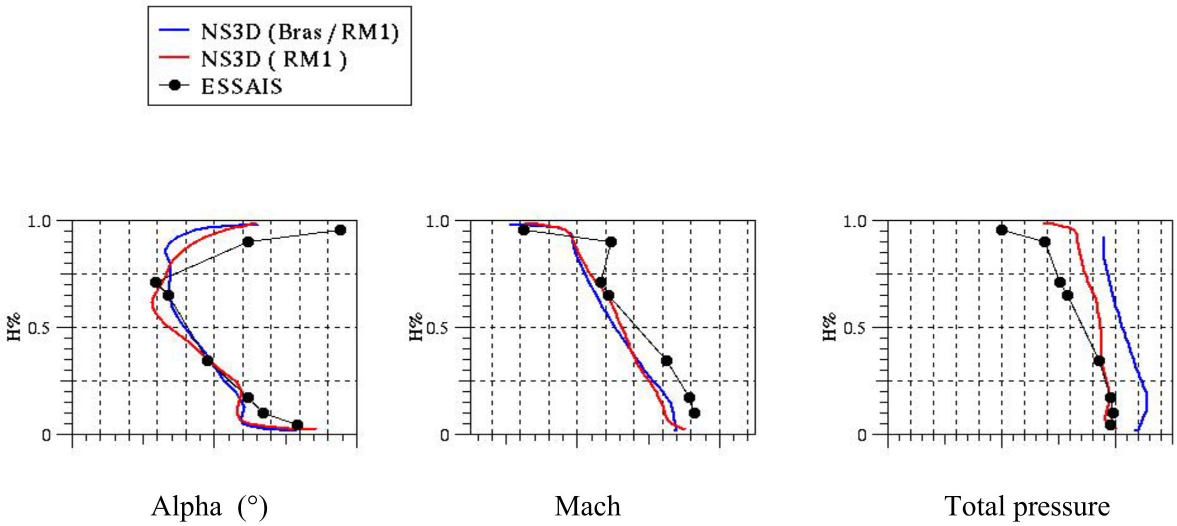

Figure 8: Calibration of steady calculations (3D NS) with respect to the tests: downstream conditions (trailing edge) of the rotor.

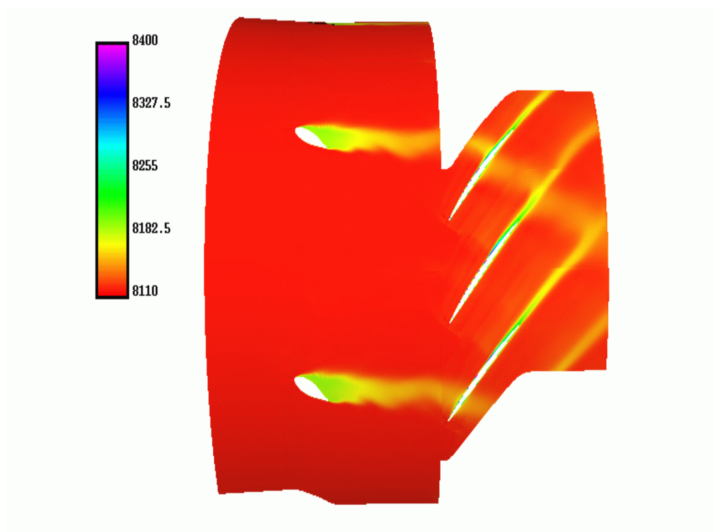

Figure 9: Iso-entropy obtained from the unsteady 3D NS calculation at 90% of the aerodynamic flowpath height.

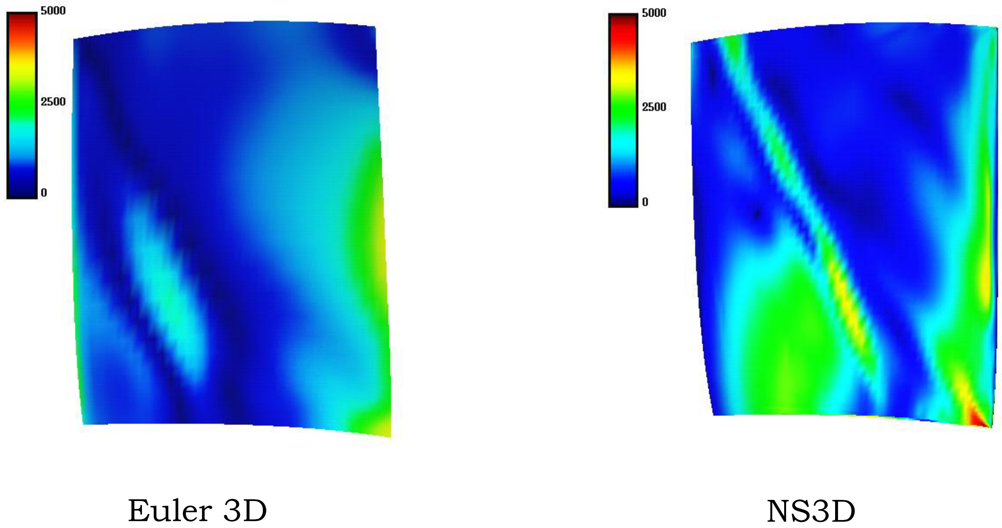

Figure 10: Modulus of the first harmonic of the static pressure on the suction side of the rotor blade obtained by 3D Euler and 3D NS calculation.

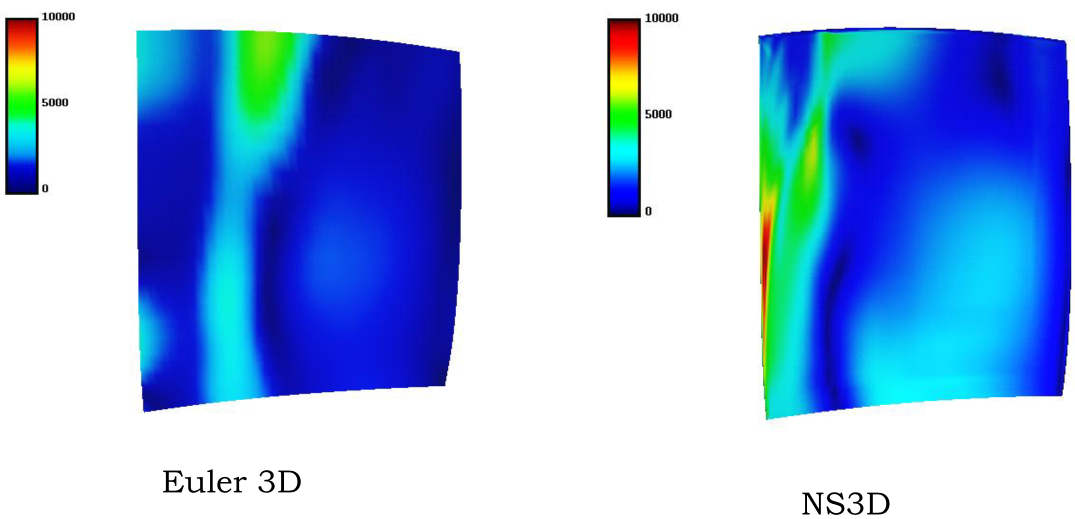

Figure 11: Modulus of the first harmonic of the static pressure on the pressure side of the rotor blade obtained by 3D Euler and 3D NS calculation.

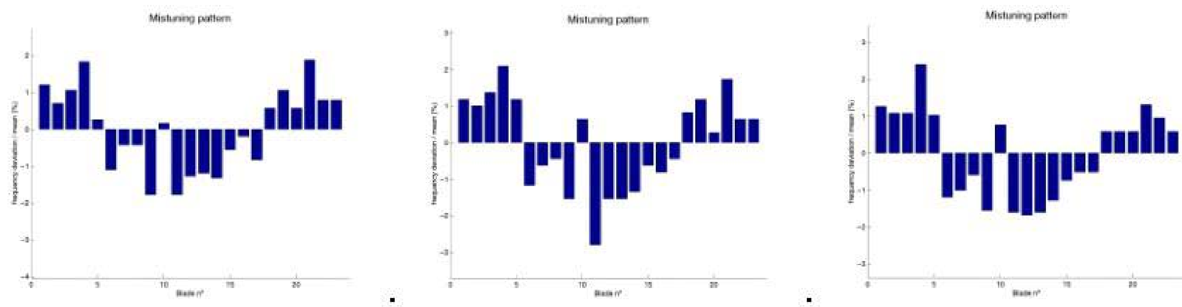

Figure 12: Mistuning patterns identified on the 3rd mode during partial tests at different stages of instrumentation.

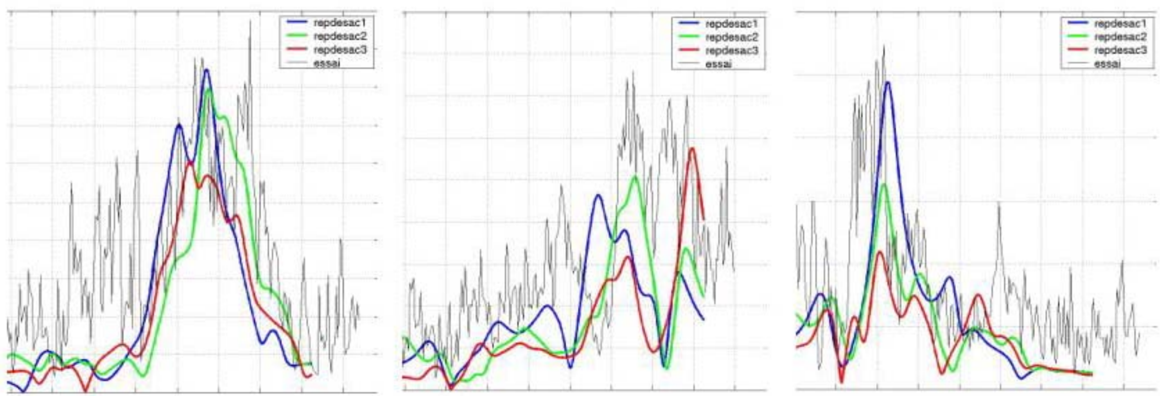

Figure 13: Sensitivity of the forced responses to mistuning, calculated from the 3 patterns identified in the partial tests.

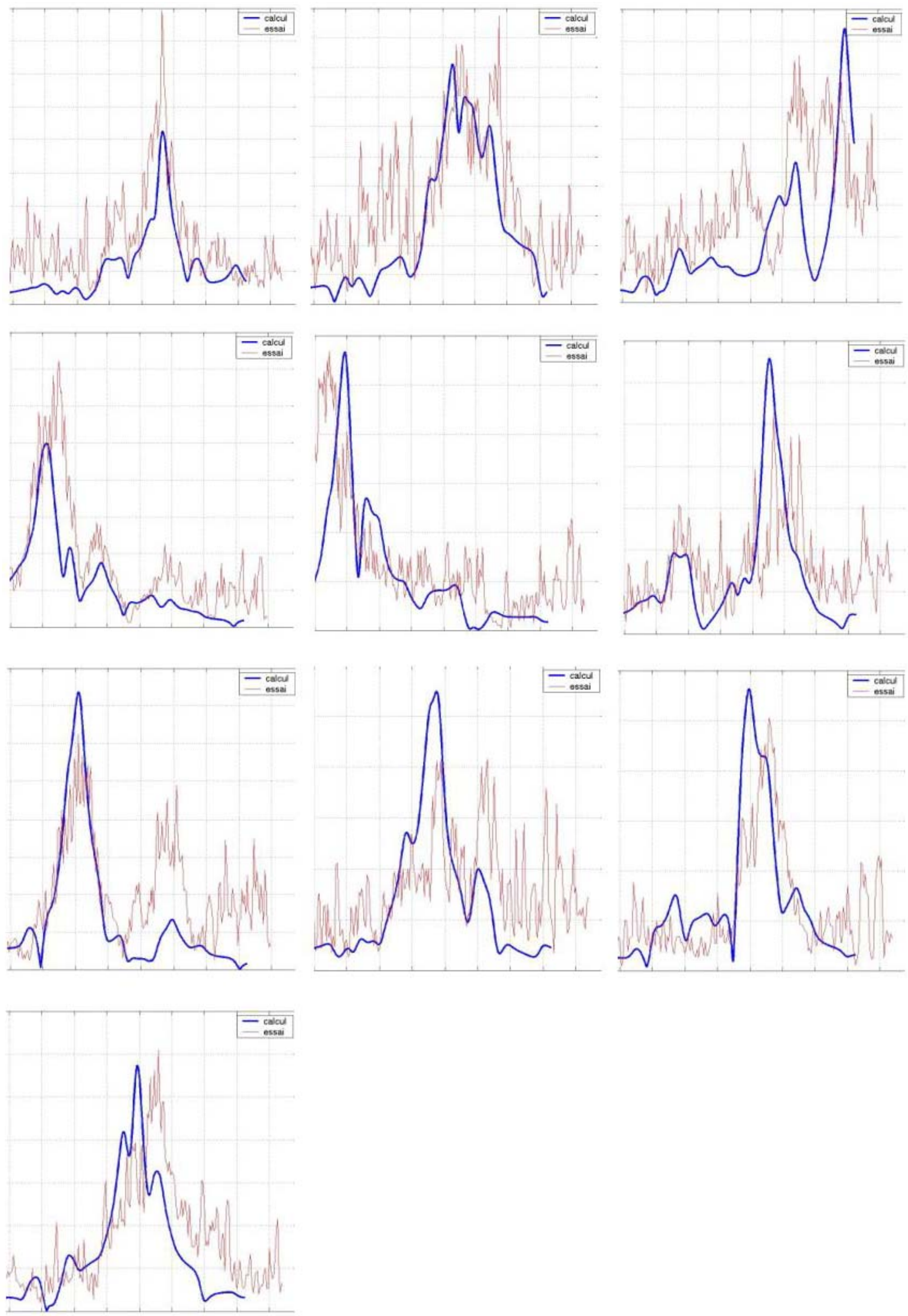

Figure 14: Correlation calculations / tests in forced response on 10 blades with the same rotating speed range (x-coordinate: rotating speed, y-coordinate: strain).

SYMPOSIA DISCUSSION – PAPER NO: 28

Author's name: J.P. Lombard

Discussor's name: A. Von Flotow

Question: Did you adjust the damping based upon test results?

Answer: Yes. Mechanical damping was measured. Aeroelastic damping was computed and the computed aeroelastic damping was reduced, based upon test results.